

**This is the accepted manuscript version of the contribution published as:**

van Gelder, S., Röhrig, N., **Schattenberg, F.**, Cichocki, N., Schumann, J., Schmalz, G., Haak, R., Ziebolz, D., **Müller, S.** (2018):  
A cytometric approach to follow variation and dynamics of the salivary microbiota  
*Methods* **134–135**, 67 - 79

**The publisher's version is available at:**

<http://dx.doi.org/10.1016/j.ymeth.2017.08.009>

# A cytometric approach to follow variation and dynamics of the salivary microbiota

Susanna van Gelder<sup>1a</sup>, Nicola Röhrig<sup>1a</sup>, Florian Schattenberg<sup>2</sup>, Nicolas Cichocki<sup>2</sup>, Joachim Schumann<sup>2</sup>, Gerhard Schmalz<sup>1</sup>, Rainer Haak<sup>1</sup>, Dirk Ziebolz<sup>1b</sup>, Susann Müller<sup>2b</sup>

<sup>1</sup> Department of Cariology, Endodontology and Periodontology, University of Leipzig, Liebigstraße 12, 04103 Leipzig, Germany

<sup>2</sup> Department of Environmental Microbiology, Working Group Flow Cytometry, Helmholtz Centre for Environmental Research – UFZ, Permoserstr. 15, 04318 Leipzig, Germany

- a) These authors are equally contributing first authors.
- b) These authors are equally contributing senior authors.

Corresponding author: susann.mueller@ufz.de

Keywords: saliva, mouth microbiome, microbial flow cytometry, cell counting, microbial diversity

## Abstract

Microbial flow cytometry is an established fast and economic technique for complex ecosystem studies and enables visualization of rapidly changing community structures by measuring characteristics of single microbial cells. Cytometric evaluation routines are available such as flowCyBar which are useful for automatic data processing. Here, a cytometric workflow was established which allows to routinely analyze salivary microbiomes on the example of ten oral healthy subjects. First, saliva was collected within a 3-month period, cytometrically analyzed and the evolution of the microbiomes followed as well as the calculation of their intra- and inter-subject similarity. Second, the respective microbiomes were stressed by exposition to high sugar or acid concentrations and immediate changes were recorded. Third, bactericide solutions were tested on their impact on the microbiomes. In all three set ups huge intra-individual variations in cytometric community structures were found to be largely absent, even under stress, while inter-individual diversity was obvious. The bacterial cell counts of saliva samples were found to vary between  $3.0 \times 10^7$  to  $6.2 \times 10^8$  cells per sample and subject in undisturbed environments. The application of the two bactericides did not cause noteworthy diversity changes but the loss in cell

numbers by about 50% was high after treatment. Illumina® sequencing of whole microbiomes or sorted sub-microbiomes revealed typical phyla such as *Firmicutes*, *Proteobacteria*, *Actinobacteria*, *Bacteroidetes* and *Fusobacteria*. This approach is useful for fast monitoring of individual salivary microbiomes and automatic calculation of intra- and inter-individual dynamic changes and variability and opens insight into ecological principles leading to their sustainment in their individual environment.

1. Introduction
  2. Material and Methods
    - 2.1. Subjects
    - 2.2. Sample collection
    - 2.3. Sample fixation
    - 2.4. Cell staining
    - 2.5. Flow cytometry
    - 2.6. Cell counting
    - 2.7. Cell sorting
    - 2.8. Data analysis
    - 2.9. Data evaluation
    - 2.10. Sequencing
    - 2.11. Controls
  3. Results and Discussion
    - 3.1. Workflow
    - 3.2. Person dependent oral microbiota
    - 3.3. Oral microbiota and stress
    - 3.4. Mouth-rinses and cell numbers
  4. Conclusion
- Acknowledgements
- References
- Figure description
- Appendix A. Supplementary material

## 1. Introduction

Microorganisms tend to assemble to complex three-dimensional structures in which they are spatially organized as intimately interacting microbial communities. Embedded in an exo-polysaccharide-matrix these constructs form biofilms [1–4]. They are ubiquitous and can grow on natural as well as artificial surfaces [5]. The oral cavity as a highly organized ecological system provides all conditions to enable the indigenous bacteria to form and mature such complex structures [1,3,6]. Currently, roughly 700 phylotypes have been detected in the oral bacterial microbiome. Species can be characterized by being specific for a site (e.g. tongue, palate, buccal mucosa, tonsils, plaque) as well as promoting health or disease [7–9].

Multitudes of modulating factors like varying bacterial and molecular interactions, micro-geographical characteristics (protective niches), nutrient availability, diet and host defense cause a heterogeneous ecosystem within the oral cavity which is further supported by distinct micro-niches [4,6,10–12]. High dynamics within this system can be assumed as microorganisms adapt rapidly to altering environmental conditions because of the generally short generation times of microorganisms under such growth supporting conditions [13]. Caries and periodontitis, as the most common oral pathologies are classic examples for primarily biofilm-related diseases but are in entirety multifactorial conditioned [1,4,14,15]. Not the appearance of single pathogens (specific infection) is responsible for the etiology of these oral diseases but the disturbance of the oral homeostasis that triggers the predominance of facultative pathogenic species (opportunistic infection) [16,17].

The homeostasis of the oral cavity is preserved by saliva [18,19]. It is an elementary part of this environment and the substance that links the different niches [20]. Therefore it provides a representative analysis medium for the global assessment of the oral microbiome [21–23]. The examination of the salivary microbiome is greatly relevant since it serves as a reservoir of the overall oral microbiota in its planktonic phase. Saliva as the planktonic suspension mirrors changes that are associated with oral diseases, like caries, gingivitis and periodontitis [9,21–25]. It is indispensable to investigate the salivary microbiome of the healthy in its entirety before shifts that promote oral diseases are detectable [7]. An advantage of analyzing the saliva is its simple, non-invasive and economical collection [19,26].

The study of oral microbial communities has changed from the first report of it by Leeuwenhoek in 1676 using single-lens microscopy [27] to the characterization using the current molecular biology techniques. Fluorescence in situ hybridization (FISH) enables a direct, simultaneous surveillance of bacterial taxa, but is confined to a few species [28,29]. The present gold standard for analyzing human microbiomes

diversity are sequencing methods. Based on these techniques a large-scale project including approximately 200 healthy subjects was launched with the result of the human oral microbiome database (HOMD) with global information on approximately 700 bacterial species detected in the oral cavity [30]. However, sequencing is still time and labor intensive. Another approach for analyzing complex ecosystems in a fast and economic way is microbial flow cytometry [31]. This is an established technique in environmental microbiology and enables the visualization of rapidly changing community structures in cytometric histograms [13,32,33]. For the evaluation of the microbial cytometric data bioinformatic tools such as Cytometric Barcoding (flowCyBar) are available that allow a nearly automatic interpretation of the data [13,34].

Aim of this study was to establish a cytometric protocol for the analysis of saliva microbiota to enable fast monitoring of changes in and between diverse microbiota. Thus, the project focused on balance or dys-balance, rather than qualitative, taxonomic composition. Existing bioinformatic evaluation pipelines were tested for their resolution depth and their ability to reveal saliva community variation. Detectability of individual profiles within this methods study was hypothesized as well as the feasibility of monitoring changes during time and different stress impacts (sugar and acid, bactericide mouth- rinses).

## 2. Material and Methods

### 2.1. Subjects

Ten subjects with the following inclusion criteria were selected for the study: representing both genders, ranging in age from 21 to 40, and with no signs of oral disease. The subjects were examined orally prior to sampling and did not have any active caries lesions, nor showed any signs of periodontal diseases. During the examination, a general anamnesis was recorded, which assessed the presence of any general diseases, medications or further oral health related parameters (e.g. smoking habits). Furthermore, a dental examination using the decayed-, missing- and filled-teeth status (DMF-T) was performed to detect carious teeth showing a cavitation of the surface (D-T). Furthermore, the PSR/PSI was executed, which detects periodontal probing depth and bleeding on probing and thus reflects the periodontal treatment need. Exclusion criteria were: general diseases, antibiotic treatment six months prior to and during sample collection or any medication that could influence the saliva secretion. Instructions of the subjects regarding the individual oral hygiene were given. For detailed information see Supplementary material Table S1. Each experiment was run twice (for the results of the second run see Supplementary material Fig. S3–S5). The study was approved by the ethics committee of the medical faculty of the University of

Leipzig, Germany (069/17-ek). All participants were informed verbally and in writing about the study and gave their written informed consent.

Trouble shooting: Different oral hygiene habits (techniques, frequency), dissimilarity of oral health state, subjects' eating habits, lack of examination of intimate partners, current respiratory tract infections

## 2.2. Sample collection

The subject was instructed to carry out the last oral hygiene procedure until 12 am of the day before collection, unless otherwise indicated. One hour (h) prior to the sample collection, the subject was asked to refrain from eating and drinking. The collection of saliva samples was conducted in accordance to the standardized spitting method protocol by Navazesh, 1993 [35]: The subject was seated comfortably for a rest of five minutes to adapt to the situation. After a mouth rinse with distilled water for 30 seconds the 5-min-collection period for unstimulated saliva followed. The subject was instructed to minimize orofacial movements during this time. The whole saliva was spit into a sterile graduated test tube on ice. Unstimulated saliva was collected to minimize potential impacts of additional process steps and due to reduced costs of materials for saliva-stimulating agents (e.g. paraffin).

Trouble shooting: Lacking certainty of following all guidelines given in the test design, unintentional stimulation of saliva, increased/decreased rate of secretion (stress, fluid intake, temperature etc.), loss of sample material (accidental swallowing, missing the collecting tube)

Reagents: crushed ice, distilled water, collection tubes (Corning, New York, USA)

## 2.3. Sample fixation

Sterile, cooled glycerol as cryoprotective agent was added to the saliva samples in a concentration of 15 % (v/v). After 10 min incubation time on ice and division into 2-3 aliquots the samples were shock frozen in liquid nitrogen and afterwards stored at -80°C.

Trouble shooting: Inaccuracy of volume determination (disruptive element: foam), heterogeneity of saliva, non-compliance with time and temperature requirements

Reagents: sterile, cooled glycerol, crushed ice, liquid nitrogen

## 2.4. Cell staining

Deep frozen and glycerol fixed saliva samples were put on crushed ice to defrost. The optical density (OD) of the cells was adjusted to 0.1 ( $d_{\lambda 700nm} = 0.5 \text{ cm}$ ) with PBS (6 mM  $\text{Na}_2\text{HPO}_4$ , 1.8 mM  $\text{NaH}_2\text{PO}_4$ , 145 mM NaCl with bi-distilled  $\text{H}_2\text{O}$ , pH 7) and well mixed. After centrifugation of 2 ml of this solution for 10 min at 4°C and 3,200 g the supernatant was discarded. The cell-pellet was resuspended in 0.5 ml of

permeabilization buffer (0.1 M citric acid, 4.1 mM Tween 20, bi-distilled water) and incubated for 20 min at room temperature. After a further centrifugation step the supernatant was discarded and the cells were resuspended in 1 ml DNA staining solution (0.68  $\mu$ M 4',6-di-amidino-2-phenyl-indole (DAPI, Sigma-Aldrich, St. Louis, USA), in 417 mM  $\text{Na}_2\text{HPO}_4/\text{NaH}_2\text{PO}_4$  buffer (289 mM  $\text{Na}_2\text{HPO}_4$ , 128 mM  $\text{NaH}_2\text{PO}_4$  with bi-distilled  $\text{H}_2\text{O}$ , pH 7)) for subsequent staining overnight at 6°C until cytometric measurement. A biological standard (*Escherichia coli* BL21 (DE3), stationary phase of growth curve (16 hs cultivation time), fixed with PFA (2%)/ EtOH (70 %)) was stained as above except the OD was adjusted to 0.035 ( $d_{\lambda 700\text{nm}} = 0.5 \text{ cm}$ ).

Trouble shooting: Pipetting inaccuracies, processing aberrations and inhomogeneity due to high viscosity of saliva, instability of the cell-pellet, disruptive factors (big human cells, extrinsic soiling)

Reagents: PBS, permeabilization buffer, DNA staining solution, biological standard (UFZ strain collection, Germany), crushed ice

## 2.5. Flow Cytometry

Cytometric data were generated using the MoFlo Legacy cell sorter (Beckman-Coulter, Brea, California, USA). It is equipped with two lasers. The blue laser Genesis MX488-500 STM OPS (Coherent, Santa Clara, California, USA) (488nm, 400mW) was used to determine the forward scatter (FSC; bandpass filter 488nm  $\pm$  5nm, neutral density filter 1.9) which is an optical characteristic containing information related to cell size and the side scatter (SSC; bandpass filter 488nm  $\pm$  5nm, neutral density filter 1.9, trigger signal) an optical characteristic containing information related to cell density. The UV laser Xcyte CY-355-150 (Lumentum, Milpitas, California, USA) (355nm, 150mW) was used for exciting the DAPI fluorescence (bandpass filter 450nm  $\pm$  32.5nm), an optical characteristic that is used for quantification of cellular DNA-content. Photomultiplier tubes were purchased from Hamamatsu Photonics (Models R928 and R3896; Hamamatsu City, Japan). The fluidic system was run at 56 psi (3.86 bar) with sample overpressure at maximum 0.3 psi and a 70  $\mu$ m nozzle. The sheath fluid was composed of 10x Sheath buffer (19 mM  $\text{KH}_2\text{PO}_4$ , 38 mM KCl, 166 mM  $\text{Na}_2\text{HPO}_4$ , 1.39 M NaCl with bi-distilled  $\text{H}_2\text{O}$ ) diluted with 0.1  $\mu$ m filtrated bi-distilled  $\text{H}_2\text{O}$  to a 0.2x working solution (for cell sorting: 0.5x working solution). Prior to all measurements, daily and in-between-day calibration of the instrument was performed linearly with 1  $\mu$ m blue fluorescent beads (FluoSpheres F8815 (350/440), lot no.: 69A1-1) and 2  $\mu$ m yellow-green fluorescent beads (FluoSpheres F-8827 (505/515), lot no.: 1717426), both from Molecular Probes (Eugene, Oregon, USA). Blue fluorescent beads (0.5  $\mu$ m and 1  $\mu$ m, both Fluoresbrite BB Carboxylate microspheres, (360/407), lot no.: 552744 and 499344, PolyScience, Niles, Illinois, USA) were used for calibration of logarithmic scale and added to each sample for measurement stability. A biological

standard (*Escherichia coli* BL21 (DE3)) was measured as a biological adjustment. The stained samples were filtered using 50 µm CellTrics filter (Sysmex Partec GmbH, Görlitz, Germany) before measurement to prevent clogging of the cytometer nozzle. By measuring the samples, logarithmically scaled 2D-dot plots with FSC (cell size) against DAPI-fluorescence (chromosome content) as parameters were generated (Fig. 1). During these measurements, a parent gate has been created in Summit 4.3 (Beckman-Coulter, Brea, CA) comprising all stained cells and excluding noise and beads. Every sample was measured at a maximum speed of 3,000 events/s until 150,000 cells within this parent gate were detected. Raw cytometric data can be found under: <https://flowrepository.org/id/RvFrzrE6fOGuSmf7NqWmPVGky1rKfqFnB3hXuii6qghQ63b9PDJPM8qlxRqEQZW>

Trouble shooting: Precipitation of the buffer, air-bubbles in the system, insufficient sample amount, high sample intrinsic noise

Reagents: 1 µm and 2 µm yellow green fluorescent beads, 0.5 µm and 1.0 µm blue fluorescent beads

## 2.6. Cell counting

Cell numbers of the cell suspensions were determined by SYBR GreenI staining of DNA to stain all cells. In comparison to DAPI staining no centrifugation steps are necessary to avoid cell loss. Staining was performed using OD 0.1 ( $d_{\lambda 700nm} = 0.5$  cm) adjusted sample suspensions, which were filtered using 50 µm CellTrics filter (Sysmex Partec GmbH, Görlitz, Germany). 925 µl filtered sample solution were stained with 50 µl 100 % ethanol (working concentration 5 %) and 25 µl 20x SYBR GreenI solution (working concentration 0.5x) (ThermoFisher Scientific, Waltham, Massachusetts, USA) for at least 30 min. 1 µm yellow-green fluorescent beads (FluoSpheres F-13081 (505/515), lot no.: 63B2-1, Molecular Probes (Eugene, Oregon, USA)) with a microscopically determined concentration were added to the staining solution prior to measurement. SYBR GreenI was excited at 488 nm with the Genesis MX488-500 STM OPS laser and logarithmically scaled 2D-dot plots with red (bandpass filter 670nm ± 15nm) against green fluorescence (bandpass filter 530nm ± 20nm) were created according to Hammes et al., 2012 [36]. Gates to determine cells and beads were created (Supplementary material Fig. S1) and cell counts/ml calculated as follows:

$$\text{Cell number ml}^{-1} = \frac{f \cdot C(\text{parent}) \cdot B \cdot V}{B(\text{YG}) \cdot V(\text{sample})}$$

*f*: Dilution rate of sample for counting

*C*(parent): Virtual cell number in the parent gate

*B*: Defined concentration of 1 µm yellow-green fluorescent beads

$V$ : Volume of defined concentration 1  $\mu\text{m}$  yellow-green fluorescent beads

$B(\text{YG})$ : Number of beads in the gate 1  $\mu\text{m}$  yellow-green fluorescent beads

$V(\text{sample})$ : Defined volume of DNA-stained cells sample

Cell count/sample volume was determined using the estimated sample volume.

Trouble shooting: Pipetting inaccuracies, processing aberrations and inhomogeneity due to high viscosity of saliva

Reagents: Ethanol (100%), SYBR GreenI solution, 1  $\mu\text{m}$  yellow-green fluorescent beads

## 2.7. Cell sorting

The cell sorting procedure was done according to the protocol by Koch, 2013 [33]: A representative number of samples were chosen under the premise of comprising 500,000 cells per gate and selected for sorting. The most accurate sort mode of the MoFlo (single and one-drop mode: highest purity 99 %) at a rate not higher than 2,500 events/s was adjusted. After sorting, cells were harvested by a centrifugation step (20,000 g, 4°C, 25 min), and the pellet was frozen at -20 °C for later DNA isolation and Illumina® sequencing. For detailed information regarding the chosen samples and gates, see Supplementary material Table S4.

Trouble shooting: Insufficient sample amount, precipitation of the buffer, air-bubbles in the system, high sample intrinsic noise, insufficient cooling due to long sorting time of low abundant gates, loss of cells by centrifugation after sorting, cell disruption of vulnerable cells during sorting

Reagents: 1  $\mu\text{m}$  and 2  $\mu\text{m}$  yellow-green beads, 0.5  $\mu\text{m}$  and 1.0  $\mu\text{m}$  blue fluorescent beads

## 2.8. Data analysis

The measurements of each sample were visualized with Summit 4.3 (Beckman-Coulter, Brea, CA) and FlowJo V10 (FlowJo, LLC, Oregon USA) using the dot-plot option FSC (cell size) against DAPI fluorescence. Subsequently, a cell gate bearing to the already defined parent gate in Summit has been defined in FlowJo excluding noise and beads (Fig. 1, A). Events within the resulting 2D-histogram can be interpreted as recorded virtual cells whose optical characteristics are represented by chosen parameters such as FSC and DAPI fluorescence. Those with similar optical properties are consequently clustered and defined as subcommunities. Visible differing clusters were marked with separate ellipsoid gates. Previous studies revealed that subcommunities may consist of only single or few phylotypes but can also contain a huge variety of phylotypes [31]. The more precisely one gate is defined the higher is the probability that one

single genus dominates this gate in a high percentage. Nevertheless, the gate must be designed with a tolerance for biological deviations within the sample pool. It must be valid for all samples within the setup of samples that needs to be evaluated together. All gates of all samples in their entity generated the gate template (Fig. 1, B), which consists of 37 gates in this study.

Trouble shooting: Operator and experience dependent (individual gating procedure according to Günther et al., 2015 [37]), necessary compromises by creating the mastergate due to biological variations and technical sensibility that cause deviation, missing of low abundant species

## 2.9. Data evaluation

Gates of interest can be compared regarding the recorded events that correspond to the virtual cell abundance. All gate values from each sample were extracted using FlowJo, saved as an Excel file and transformed into a text file. These data are normalized and can be used by flowCyBar [38] to create unique barcodes (Fig. 2, A), where every bar/column corresponds to one specific gate and every row corresponds to one sample. This procedure is called cytometric fingerprinting [33]. In Fig. 2, A the samples were put together in four different groups. A color key gradient displays the variation of the normalized gate abundances (Fig. 2, A): dark blue corresponds to low and red to high virtual cell abundance compared to the average of the appropriate gate. The average of virtual cells per gate is indicated by white color. Thus, the barcode shows an in-/decrease of gate-cell abundances, but no interpretation of the cells' percentage in this specific gate. On the top of each barcode a cluster dendrogram illustrates the clustering of all gates as a result of a hierarchical approach using the Euclidian metric. A second depiction of the cytometric data is possible by creating boxplots that show the distribution of the relative abundances of gate cell numbers of each gate (Fig. 2, B).

Furthermore, non-metric multidimensional scaling (NMDS) was performed based on the relative gate cell abundances of all samples. The distance measure used for this approach was the Bray-Curtis dissimilarity. The NMDS plots were created using the nmds method of the R package flowCyBar [38] which is based on the metaMDS method of the R package vegan [39]. The distance between two points/samples describes their (dis-) similarity (Fig. 2, D and E). Thus, two samples with high similarity are ordinated closer together than those with a low similarity. All dynamics of an oral community can be illustrated representing the direction of the evolution of samples over time (Fig. 2, D). The similarity or dissimilarity of a defined group of samples is mirrored by the deviation between all points of this group (Fig. 2, E). Consequently, larger deviations between points represent high dissimilarity between samples. In Fig. 2, E two sample groups were defined and connected by a solid line. Instead of connecting the points of one group it is also possible to add ellipsoid lines showing the standard deviation of this group.

Trouble shooting: over-interpretation of distances due to lacking standard gradation of NMDS-plots

## 2.10. Sequencing

The workflow for the sequencing procedure is presented in detail in the Supplementary Appendix (Supplementary material, pages 4-7). Several steps need to be undertaken starting with the creation of mock strains and a mock community for control, DNA extraction and quality testing, library preparation for Illumina® sequencing, and finally, the sequencing data evaluation procedure.

## 2.11. Controls

### 2.11.1. Technical replicates

The reliability of cytometric measurements was assured by creating technical replicates. A possible impact of the cytometric workflow can cause variation in measured data sets. To ensure a minimum of possible influences connected to protocols or equipment independent measurements of the same sample were performed. Therefore, one sample was split into three parts and processed separately according to the cytometric workflow and each was measured three times. Their dissimilarity is extremely slight as shown in Fig. 3 (TR).

### 2.11.2. Fixation stability

Fixation of samples is a critical issue in order to keep the cells in stasis at a particular point and to avoid deterioration. In this study, N<sub>2</sub> fixation (Glycerol 15% (v/v), -80°C; see 2.3 Sample fixation) was used to stabilize and fix all cells, because after testing two further different fixatives (N<sub>2</sub>, Glycerol 15% (v/v), -20°C and formaldehyde/alcohol (PFA 2% / EtOH 70%) it showed the highest quality preservation. The stability was tested for up to 135 days, using flow cytometry. A sample was repeatedly prepared and analyzed at different measuring days to ensure the comparability of measurements. The fixation stability was proven as shown in Fig. 3 (FIX) and a high similarity between all samples was discernible.

### 2.11.3. Negative controls

Negative controls of the used products were performed to ensure that a measured change in community structure is not caused by these products and that they do not perform a distortion on the measured events within the cell gate. Therefore, PBS buffer, the tooth brushes Elmex inter X mittel (GABA Group, Therwil, Swiss) and Sensodyne Mikro Aktiv extra sanft (GlaxoSmithKline plc., London, Great Britain), the tooth pastes Sensodyne Multicare (GlaxoSmithKline plc., London, Great Britain) and Meridol (GABA Group, Therwil, Swiss), and the mouth rinses Listerine® Total Care Clean Mint (Johnson & Johnson, New

Brunswick, USA) and Dynexan Proaktiv 0,2% CHX (Kreussler Pharma, Wiesbaden-Biebrich, Germany) were proceeded according to the cytometric workflow. The contribution of the stained particles to the events of the defined cell gate was found to be not significant. For further information see Supplementary material Fig. S2.

Trouble shooting: Determination of the maximum amount of product that one saliva sample could contain

Reagents: PBS buffer

#### 2.11.4. Sorting controls

To exclude possible distortions by the sorting procedure one sample was split. One part was sequenced directly, the other part after cytometric measurements. Only slight differences became apparent (Fig. 9, D).

Trouble shooting: See 2.7. Cell sorting and workflow for Illumina® sequencing

## 3. Results and discussion

### 3.1. Workflow

A summary of the performed experiments as well as the cytometric workflow is illustrated in Fig. 4. Unstimulated saliva samples were collected from ten oral healthy subjects. Three different experiments were designed, including a long-term experiment where the variations of the respective personal microbiota were followed over three months; a short-term experiment where the influence of both free-sugar containing sweets (represented by Toffifee (Storck, Berlin, Germany)) and dietary acid soft drinks (represented by Coca Cola Zero (The Coca-Cola Company, Atlanta, USA)) on the microbiota was tested; and finally two bactericide solutions were imparted and their impact on the microbiota analyzed. After sampling and fixation, the samples were processed immediately or to a later time point. Fixation stability was tested and found stable for up to 135 days (Fig. 3, FIX). Washing and DNA-staining of the samples was followed by flow cytometric community analysis. Subsequently, the generated data were evaluated by using bioinformatic tools. Although this workflow has been used to investigate samples from different environments in the past, it has never been used for saliva before. The number of cells per ml saliva is rather low (3.4 Mouth-rinses and cell numbers; Supplementary material Table S2 & S3) which is different for e.g samples from a wastewater treatment plant [40,41] or mice feces [31]. In addition, the observed appearance of human cell debris after biocide treatment (not shown) and the viscous consistency of the

saliva that contained a certain particle matrix needed a particular careful sample handling such as a new fixation technique, parallel sample testing, surplus control set ups and creation of a specific parent gate that contained all stained cells excluding noise and beads (2. Material and Methods). Therefore, the reliability of the workflow was proven by the successful formation of almost identical cytometric community patterns of three parallels (including fixation, washing and staining) which were measured three times each (Fig. 3, TR).

### 3.2. Person dependent oral microbiota

There have been several studies to investigate the human oral microbiome by sequencing approaches [7,24,25,30,42,43]. The human oral microbiome project (HOMP) [30,43] studied seven intra-oral and two oropharyngeal sites from approximately 200 healthy donors and created a vast database (<http://www.homd.org/>). It covers 185-322 bacterial genera belonging to 13-19 phyla, of which *Firmicutes*, *Bacteroidetes*, *Proteobacteria*, *Fusobacteria* and *Actinobacteria* were the most dominant ones. The project revealed that saliva as one oral habitat showed the highest median alpha-diversity but one of the lowest beta-diversities. The total number of organisms (richness of measured OTU (operational taxonomic unit) numbers) and/or the respective relative abundances of organisms (evenness) within a sample were used to characterize alpha-diversity. Beta-diversity in contrast describes the comparison between samples from the same habitat among subjects. Hence, concerning saliva samples, the measured OTU level richness within one sample was described to be high, but samples of different subjects shared similar organisms [30,43]. Moreover, when it comes to time-linked saliva community studies it seems that intra-individual variation occurred only subtly but differed in succession from other saliva microbiome structures [44]. Also other studies found that samples collected over longer intervals were more similar, while those taken at shorter intervals were often more dissimilar as possible deviation from the normal state was regarded with higher weight [9,30]. Such data point to the existence of a highly diverse 'personal microbiome' that undergoes only modest fluctuations when it is not heavily affected.

Using the cytometric workflow, the findings of the long-term experiment in the current study (details in Supplementary material Table S1) correspond to the findings discussed before [9,30,43,44]: Subject specific microbiome patterns showed intra-individual constancy but were different between each other, although partly overlapping in similarity, thus revealing inter-individual diversity (Fig. 5, S6). Samples of some of the subjects showed an especially high constancy over time (e.g.: subjects 6 and 10), as their respective microbiomes are arranged closely together within the dissimilarity matrix. The salivary microbiota of others showed less permanent patterns within this 3-month period (e.g.: subjects 3 and 8;

also revealed by an independent parallel set up represented in Fig. S3). To statistically confirm the findings an ANOSIM test was performed based on the cytometric gate abundances of all 10 subjects for the long-term experiments. *R* values of approx. 0.5 describe higher inter-individual than intra-individual variance with a significance value of 0.001 for the first long-term experiment and for the parallel set up (S6A, S7A). Notched boxplots were created to visualize these test results (S6A, S7A). To confirm the cytometric measurements and the obtained community structure information, Illumina® sequencing was performed exemplarily of two samples from the microbiome of subject 1 taken with a time delay of three weeks. Only few changes in abundance were observed by an increase of 15 to 22 OTUs and 10 to 16 genera between the two samples. All 10 genera found in week 1 were also present in week 4 and the other 6 genera increased in abundance to only about 1% each (Fig. 9, A). The genus *Prevotella* was more than 2 times more abundant in the sample taken at 7 days while e.g. the genus *Neisseria* was about 4 times more abundant at the 4 week-sampling. In contrast to the microbiome of subject 1, the sequencing data of other microbiomes (subjects 6 and 10) showed more different compositions of the OTU types although both were taken at the same time point (see Fig. 9, A). *Lachnospiraceae* were only represented in the sample of subject 6 while *Brevundimonas* as well as *Lactococcus* were found only in the sample of subject 10. Other phylotypes detected in both samples were represented in different abundancies, for example *Prevotella* was more abundant in the sample of subject 6. The difference in the OTU types and abundance between the three microbiomes, however, was lower as described in literature [43] due to sequencing depth, but nevertheless, also the cytometric analysis and similarity calculation positioned those three microbiomes in near vicinity (Fig. 5). Thus, the data obtained by Illumina® sequencing strongly supported the trends calculated on the basis of cytometric data by representing the high intra-individual constancy of OTU types in the microbiome of subject 1 and inter-individual diversities (variation of OTU types) of microbiomes of subjects 1, 6 and 10. The beta-diversity among the microbiomes of those three subjects was existent, but low.

### 3.3. Oral microbiota and stress

It is verified that an excessive intake of sugars and acids leads to an increased risk for oral diseases like caries and dental erosion [45–47]. This is accompanied by a microbial shift from oral homeostasis to a dysbiosis due to selection of facultative pathogenic phylotypes such as *Streptococcus spp.*, *Prevotella spp.*, *Veillonella spp.*, and *Lactobacillus* [23,48]. In healthy oral microbiomes these phylotypes are also frequently represented, but minor abundant [22,49]. Saliva serves as a protection against stress influences due to its functions as cleansing solution, buffer and source for remineralization [50,51]. A previous sequencing project revealed an association between salivary bacterial profiles and oral health

and disease, thus bacteria from local oral diseased sites are also detectable in saliva [23]. Nonetheless, the presence of such pathogenesis-associated genera does not implicitly obligatorily an existing disease. Objective of this experimental set up was to imitate a dietary lifestyle by taking up of sugars or acids several times within an 8 h period to avoid recovery of the salivary microbiome. The data of this study suggest that a short-term intensive extrinsic stress such as treatment with small molecular sugars liberated from sweets or acids from soft drinks did not change the intra-individual constancy of microbiomes that much (Fig. 6 and Supplementary material Fig. S4). ANOSIM testing for variance and significance was performed and results documented in S6B,C and S7B,C. As before, the similarity analysis showed clear differences between the microbiomes of different subjects taken at baseline (before a stress impact) similar to the microbiomes taken for the long-term experiment (see 3.1 Person dependent oral microbiota). After the stress impact (8 h) the microbiomes were still in the vicinity to their earlier position in the similarity analysis. These findings were found for the two different stress situations (influence of low molecular sugars and acids) and also the two independent experimental replicates. The data therefore suggest that the intra-individual constancy of the microbiomes seem to be a central phenomenon as the microbiomes act with high resilience and operated the stress with only slightly changed basic structures. The microbiomes did not evolve collectively to a united structure as could have been suggested by an assumed dominance of acidogenic phylotypes under such conditions. Though data in literature are controverse, most authors describe that excessive and long-term dietary sugar intake and low pH leads to a shift of the healthy oral microbiota to a decreased microbial diversity encouraging acidogenic phylotypes, such as *Streptococcus*, *Lactobacillus* and *Veillonella* [22,23,52,53]. In this study sequencing was performed exemplarily for one subject (subject 6) at baseline and after 8 h of stress impact (sugar). In addition, selected gates of the two microbiomes were sorted and sequenced (Fig. 9, B). Some gates of the baseline microbiome were dominated by key subpopulation such as gate 3 by *Prevotella* (almost 70 %) or gate 37 by *Alloprevotella* (almost 85 %). Instead of the promotion of only a few acidogenic phylotypes an increased number of phylotypes was detectable after the sugar stress impact (Fig. 9, B, 8 h). The alpha-diversity within samples increased, for example the genera *Aminobacteria*, *Lactococcus* or *Myroides* turned up. As in literature a decrease of the microbial diversity of caries disease is explained [23,52], initially these results appear controversial, yet the healthy state of the salivary microbiome of the examined subject and the short-term impact of only 8 h have to be considered. Furthermore, abundancies of phylotypes changed. An increase of the genera *Streptococcus* by the factor 3.5 is interesting, because some *Streptococcus spp.* are associated with caries pathogenesis [22,48]. Interestingly, gate 4 was mainly occupied by *Streptococcus* (37 %) but also other phylotypes were present: *Prevotella* (16 %), *Porphyromonas* (9 %), *Gemella* (8 %). However, since only one

microbiome structure under stress was resolved by Illumina® sequencing, no detection on species level was performed and, additionally, the existence of *Streptococcus spp.* does not mandatory reflects caries, no further statement regarding a potential disease etiology can be made. As stated before, the cytometric microbiome data suggested only a minor change after short term impact of sugars and acids but without affecting the general structures of the individual microbiomes that much and thus saliva seems to accomplish its function as protective reservoir of a healthy microbiome for such periods.

#### 3.4. Mouth-rinses and cell numbers

Mouth-rinses are used with the intention to reduce the microbial load in the oral cavity [54–56]. The agents contained therein are responsible for the effectiveness of meeting this requirement [54,57,58]. Mouth-wash containing 0.2 % Chlorhexidine (CHX) is well investigated for several times and its significant antibacterial effect is confirmed [59]. The cationic nature of the active substance CHX enables an adherence on anionic oral surfaces and persistence at effective concentrations. This characteristic is defined as substantivity, enabling a prolonged antibacterial activity [60,61]. This parameter can be evaluated by observing the decrease of salivary bacterial numbers over a time period. Different methods, like epifluorescence microscopy investigating bacterial vitality or cultivation on agar plates for counting colony forming units (CFU)/ml are already described in literature. The resulting findings describe an immediate potent reduction of the salivary flora after application of CHX followed by a progressive recovery in bacterial vitality, still showing an incomplete return to baseline hours later [60,62,63]. The intention of this study was to determine the absolute cell numbers by flow cytometry rather than using cultivation techniques that miss almost all the species in the microbiome due to unknown cultivation conditions. First, the cell number of microbiomes collected at baseline was determined for all subjects (Supplementary material, Table S2 & S3) by SYBR GreenI staining (2.6. Cell counting) to avoid cell loss due to washing- and centrifugation-steps that are not necessary in contrast to DAPI-staining. In addition, the cell number was determined per ml, but also per entire sample because the saliva production is a highly heterogeneous secretion process and the range of the individual saliva quantities can be wide [64]. The flow cytometric measurements provide bacterial cell numbers ranging from  $3.0 \times 10^7$  to  $6.2 \times 10^8$  per sample and  $1.5 \times 10^7$  to  $5.1 \times 10^8$  per ml in undisturbed environments. The generated data overlaps with the findings in literature [65], though comparable source material is rare. For instance, quantitative real-time PCR of bacterial counts in untreated saliva samples revealed values ranging from  $1.56 \times 10^6$  to  $1.08 \times 10^8$  cells/sample) [65]. Second, cell numbers of two subjects (subjects 6, 10) that rinsed with CHX mouth-rinse were taken before treatment (0 h) and at three time points (5 min, 2 h, 8 h) afterwards (Fig. 7). Both the cell number per entire sample and per ml decreased within 8 h

after rinsing for about 1.8 and 2.6 times (subject 6) and 1.2 and 2.1 times (subject 10), respectively, indicating a successful effect of CHX. The second run showed similar trends concerning reduction of bacterial cell counts by CHX, but it was also clear that the general abundance of cells per ml or sample varied between subjects (Fig. 7, Supplementary material Table S2 & S3, Fig. S5).

Additionally, the influence of CHX and Listerine on the cytometric structure of the salivary microbiomes of five subjects was investigated in two independent experiments, respectively (Fig. 8, Supplementary material Fig. S5). The cytometric data were grouped according to the microbiome collection times (0 h, 5 min, 2 h, 8 h). The high overlaps in all four experiments indicated that the salivary microbiomes maintained their structure despite the mouth-rinse treatment and did not collectively evolve in a united direction as could be assumed if only distinct phylotypes would survive the treatment. ANOSIM testing for variance and significance was performed and results documented in S6D,E and S7D,E. Therefore, the losses in cell number seem to be the dominant effect although some phylotypes seem to be specifically affected. Illumina® sequencing was performed exemplarily for one subject (subject 6) at baseline and 8 h after rinsing with 0.2% CHX (Fig. 9, C). Again, due to the stress situation the 8 h sample showed higher alpha-diversity with upcoming phylotypes such as *Fusobacterium*, *Neisseria* or *Rothia*, which was in contrast to the high abundancies of *Prevotella* at 0 h. The genera *Streptococcus* increased of a factor of 2-fold (from 3.5% to 6.6%) while *Prevotella* decreased by 5 times (from 48.9% to 10.6% abundance). The intention of mouth-rinse solutions is rather to cause a general and random reduction in bacterial cell counts [54,55] as was verified by the cell count measurements and the similarity comparison of the cytometric data. But shifts in microbial composition as wereobserved in this one exemplary microbiome of subject 6 with Illumina® sequencing can be dangerous because also pathogens might find unoccupied niches in a rinsed mouth ecosystem. Further studies are necessary in this regard.

## 4. Conclusion

Flow cytometry and connected bioinformatics tools visualize changes in the salivary microbiome with economic swiftness and can thus serve as screening methods preceding in depth analysis by sequencing techniques which then can be applied more selectively and only when needed. In the study, the dynamics of the saliva microbiomes of ten subjects within a 3-month period revealed individual fingerprint-like profiles with high intra-community constancy. Short term stress caused no noteworthy changes in cytometric structure of the individual microbiomes, independent if the stress was caused by sugars or acids as well as bactericides. The mouth-rinse CHX, however, caused drastic reductions in cell

counts even after 8 hs recovery time. The cytometric data suggested in general random elimination of bacteria while the sequencing data of (only) one microbiome alert also for niche colonization of formerly infrequent phylotypes. But largely, the data obtained by Illumina® sequencing, as qualitative analysis, supported the intra-community constancy especially for subject 6 because the variations in number of phylotypes and their abundancies did not changes much during all experimental set ups. Illumina® sequencing also confirmed that cells measured by flow cytometry were typical members of the salivary microbiome and that some gates might serve as indicator gates for phylotypes such as *Prevotella*.

In this study, microbiomes of healthy subjects were investigated according to particular calibration-guidelines (Supplementary material Table S1) but with no further control of nutritional habits. Therefore, additional factors (state of health, oral hygiene measures) that influence the salivary microbiome can't be excluded. Furthermore, diurnal variation could also affect the bacterial composition, but there is little or no evidence [44]. Nevertheless, under realistic clinical conditions patients are not standardized regarding these aspects either. The sparse number of included subjects requires caution, a fact that could be overcome by large-scale studies. Extended investigation of other oral niches, like periodontal pockets or the inclusion of subjects with oral diseases can yield further insights on the relation between changes of the microbial composition, community dynamics, and pathogenesis.

### **Acknowledgements**

Special thanks are given to Claudia Rüger for assistance and organization and to all subjects for their time and effort. The Sequencing was done in cooperation with Genome Analytics Group at Helmholtz Centre for Infection Research in Braunschweig (GMAK, HZI, Braunschweig, Germany). This study was supported by the Helmholtz Centre for Environmental Research (UFZ), the Central Innovation Programme for SMEs (ZIM) of the federal ministry of economic affairs and energy (BMWi) (INAR-ABOS, 16KN043222), the Federal Ministry of Education and Research (BMBF) (WiPro-Wissensbasierte Prozessintelligenz, 031A616K) and the European Regional Development Funds (EFRE – Europe funds Saxony, 100192205).

### **Appendix A. Supplementary material**

Supplementary material associated with this article can be found as online version.

## **References**

- [1] C. Bortolaia, L. Sbordone, Biofilms of the oral cavity. Formation, development and involvement in the onset of diseases related to bacterial plaque increase, *Minerva Stomatol.* 51 (2002) 187–192.

- [2] C. Hannig, M. Hannig, O. Rehmer, G. Braun, E. Hellwig, A. Al-Ahmad, Fluorescence microscopic visualization and quantification of initial bacterial colonization on enamel in situ, *Arch. Oral Biol.* 52 (2007) 1048–1056.
- [3] P.D. Marsh, Dental plaque: biological significance of a biofilm and community life-style, *J. Clin. Periodontol.* 32 (2005) 7–15.
- [4] H. Koo, M.L. Falsetta, M.I. Klein, The exopolysaccharide matrix: a virulence determinant of cariogenic biofilm, *J. Dent. Res.* 92 (2013) 1065–1073.
- [5] A.-A. Boisvert, M.P. Cheng, D.C. Sheppard, D. Nguyen, Microbial Biofilms in Pulmonary and Critical Care Diseases, *Ann. Am. Thorac. Soc.* 13 (2016) 1615–1623.
- [6] N.S. Jakubovics, Intermicrobial Interactions as a Driver for Community Composition and Stratification of Oral Biofilms, *J. Mol. Biol.* 427 (2015) 3662–3675.
- [7] J.A. Aas, B.J. Paster, L.N. Stokes, I. Olsen, F.E. Dewhirst, Defining the normal bacterial flora of the oral cavity, *J. Clin. Microbiol.* 43 (2005) 5721–5732.
- [8] R.J. Palmer JR, Composition and development of oral bacterial communities, *Periodontol.* 2000. 64 (2014) 20–39.
- [9] V. Lazarevic, K. Whiteson, D. Hernandez, P. Francois, J. Schrenzel, Study of inter- and intra-individual variations in the salivary microbiota, *BMC Genomics.* 11 (2010) 523.
- [10] N.S. Jakubovics, Saliva as the Sole Nutritional Source in the Development of Multispecies Communities in Dental Plaque, *Microbiol. Spectr.* 3 (2015).
- [11] A. Kensche, S. Basche, W.H. Bowen, M. Hannig, C. Hannig, Fluorescence microscopic visualization of non cellular components during initial bioadhesion in situ, *Arch. Oral Biol.* 58 (2013) 1271–1281.
- [12] X. Xu, J. He, J. Xue, Y. Wang, K. Li, K. Zhang, Q. Guo, X. Liu, Y. Zhou, L. Cheng, M. Li, Y. Li, Y. Li, W. Shi, X. Zhou, Oral cavity contains distinct niches with dynamic microbial communities, *Environ. Microbiol.* 17 (2015) 699–710.
- [13] C. Koch, H. Harms, S. Müller, Dynamics in the microbial cytome-single cell analytics in natural systems, *Curr. Opin. Biotechnol.* 27 (2014) 134–141.
- [14] L. Sbordone, C. Bortolaia, Oral microbial biofilms and plaque-related diseases: microbial communities and their role in the shift from oral health to disease, *Clin. Oral Investig.* 7 (2003) 181–188.
- [15] W.G. Wade, The oral microbiome in health and disease, *Pharmacol. Res.* 69 (2013) 137–143.
- [16] B. Liu, L.L. Faller, N. Klitgord, V. Mazumdar, M. Ghodsi, D.D. Sommer, T.R. Gibbons, T.J. Treangen, Y.-C. Chang, S. Li, O.C. Stine, H. Hasturk, S. Kasif, D. Segre, M. Pop, S. Amar, Deep sequencing of the oral microbiome reveals signatures of periodontal disease, *PLoS One.* 7 (2012) e37919.
- [17] P.D. Marsh, Microbial ecology of dental plaque and its significance in health and disease, *Adv. Dent. Res.* 8 (1994) 263–271.
- [18] W. van 't Hof, E.C.I. Veerman, A.V. Nieuw Amerongen, A.J.M. Ligtenberg, Antimicrobial defense systems in saliva, *Monogr. Oral Sci.* 24 (2014) 40–51.
- [19] N. Grassl, N.A. Kulak, G. Pichler, P.E. Geyer, J. Jung, S. Schubert, P. Sinitcyn, J. Cox, M. Mann, Ultra-deep and quantitative saliva proteome reveals dynamics of the oral microbiome, *Genome Med.* 8 (2016) 44.
- [20] A. Ash, P.J. Wilde, D.J. Bradshaw, S.P. King, J.R. Pratten, Structural modifications of the salivary conditioning film upon exposure to sodium bicarbonate: implications for oral lubrication and mouthfeel, *Soft Matter.* 12 (2016) 2794–2801.
- [21] J.D. Rudney, Saliva and dental plaque, *Adv. Dent. Res.* 14 (2000) 29–39.

- [22] F. Teng, F. Yang, S. Huang, C. Bo, Z.Z. Xu, A. Amir, R. Knight, J. Ling, J. Xu, Prediction of Early Childhood Caries via Spatial-Temporal Variations of Oral Microbiota, *Cell Host Microbe*. 18 (2015) 296–306.
- [23] D. Belstrøm, B.J. Paster, N.-E. Fiehn, A. Bardow, P. Holmstrup, Salivary bacterial fingerprints of established oral disease revealed by the Human Oral Microbe Identification using Next Generation Sequencing (HOMINGS) technique, *J. Oral Microbiol.* 8 (2016) 30170.
- [24] F. Yang, X. Zeng, K. Ning, K.-L. Liu, C.-C. Lo, W. Wang, J. Chen, D. Wang, R. Huang, X. Chang, P.S. Chain, G. Xie, J. Ling, J. Xu, Saliva microbiomes distinguish caries-active from healthy human populations, *ISME J.* 6 (2012) 1–10.
- [25] S. Huang, F. Yang, X. Zeng, J. Chen, R. Li, T. Wen, C. Li, W. Wei, J. Liu, L. Chen, C. Davis, J. Xu, Preliminary characterization of the oral microbiota of Chinese adults with and without gingivitis, *BMC Oral Health*. 11 (2011) 33.
- [26] J. Liu, Y. Duan, Saliva: a potential media for disease diagnostics and monitoring, *Oral Oncol.* 48 (2012) 569–577.
- [27] S. Hamarneh, Measuring the Invisible World. The life and works of Antoni van Leeuwenhoek. A. Schierbeek. Abelard-Schuman, New York, 1959. 223 pp. \$4, *Science*. 132 (1960) 289–290.
- [28] M.D. Ferrer, A. Mira, Oral Biofilm Architecture at the Microbial Scale, *Trends Microbiol.* 24 (2016) 246–248.
- [29] L. Karygianni, E. Hellwig, A. Al-Ahmad, Multiplex fluorescence in situ hybridization (M-FISH) and confocal laser scanning microscopy (CLSM) to analyze multispecies oral biofilms, *Methods Mol. Biol.* 1147 (2014) 65–72.
- [30] J.-H. Moon, J.-H. Lee, Probing the diversity of healthy oral microbiome with bioinformatics approaches, *BMB Rep.* 49 (2016) 662–670.
- [31] J. Zimmermann, T. Hübschmann, F. Schattenberg, J. Schumann, P. Durek, R. Riedel, M. Friedrich, R. Glaubien, B. Siegmund, A. Radbruch, S. Müller, H.-D. Chang, High-resolution microbiota flow cytometry reveals dynamic colitis-associated changes in fecal bacterial composition, *Eur. J. Immunol.* 46 (2016) 1300–1303.
- [32] C. Koch, F. Harnisch, U. Schröder, S. Müller, Cytometric fingerprints: evaluation of new tools for analyzing microbial community dynamics, *Front. Microbiol.* 5 (2014) 273.
- [33] C. Koch, S. Günther, A.F. Desta, T. Hübschmann, S. Müller, Cytometric fingerprinting for analyzing microbial intracommunity structure variation and identifying subcommunity function, *Nat. Protoc.* 8 (2013) 190–202.
- [34] C. Koch, I. Fetzer, H. Harms, S. Müller, CHIC-an automated approach for the detection of dynamic variations in complex microbial communities, *Cytometry A.* 83 (2013) 561–567.
- [35] M. Navazesh, Methods for collecting saliva, *Ann N Y Acad Sci.* 694 (1993) 72–77.
- [36] F. Hammes, T. Broger, H.-U. Weilenmann, M. Vital, J. Helbing, U. Bosshart, P. Huber, R.P. Odermatt, B. Sonnleitner, Development and laboratory-scale testing of a fully automated online flow cytometer for drinking water analysis, *Cytometry A.* 81 (2012) 508–516.
- [37] S. Günther, S. Müller, Facilitated gate setting by sequential dot plot scanning, *Cytometry A.* 87 (2015) 661–664.
- [38] J. Schumann, C. Koch, S. Günther, I. Fetzer, S. Müller, flowCyBar: Analyze flow cytometric data using gate information. R package version 1.12.0., 2015.  
<http://bioconductor.org/packages/release/bioc/html/flowCyBar.html>

- [39] J. Oksanen, F.G. Blanchet, M. Fiendly, R. Kindt, P. Legendre, D. McGlenn, P.R. Minchin, R.B. O'Hara, G.L. Simpson, P. Solymos, M.H.H. Stevens, E. Szoecs, H. Wagner, *vegan: Community Ecology Package*. R package version 2.4-3., 2017. <https://CRAN.R-project.org/package=vegan>
- [40] S. Günther, K. Faust, J. Schumann, H. Harms, J. Raes, S. Müller, Species-sorting and mass-transfer paradigms control managed natural metacommunities, *Environ. Microbiol.* 18 (2016) 4862–4877.
- [41] S. Günther, C. Koch, T. Hübschmann, I. Roske, R.A. Müller, T. Bley, H. Harms, S. Müller, Correlation of community dynamics and process parameters as a tool for the prediction of the stability of wastewater treatment, *Environ. Sci. Technol.* 46 (2012) 84–92.
- [42] F. Yang, K. Ning, X. Chang, X. Yuan, Q. Tu, T. Yuan, Y. Deng, C.L. Hemme, J. van Nostrand, X. Cui, Z. He, Z. Chen, D. Guo, J. Yu, Y. Zhang, J. Zhou, J. Xu, Saliva microbiota carry caries-specific functional gene signatures, *PLoS One.* 9 (2014) e76458.
- [43] Human Microbiome Project Consortium, Structure, function and diversity of the healthy human microbiome, *Nature.* 486 (2012) 207–214.
- [44] D. Belstrøm, P. Holmstrup, A. Bardow, A. Kokaras, N.-E. Fiehn, B.J. Paster, Temporal Stability of the Salivary Microbiota in Oral Health, *PLoS One.* 11 (2016) e0147472.
- [45] P.A. Belardinelli, R.A. Morelato, T.E. Benavidez, A.M. Baruzzi, S.A. Lopez de Blanc, Effect of two mouthwashes on salivary pH, *Acta. Odontol. Latinoam.* 27 (2014) 66–71.
- [46] P. Moynihan, P.E. Petersen, Diet, nutrition and the prevention of dental diseases, *Public Health Nutr.* 7 (2004) 201–226.
- [47] A. Sheiham, Dietary effects on dental diseases, *Public Health Nutr.* 4 (2001) 569–591.
- [48] N. Takahashi, Oral Microbiome Metabolism: From "Who Are They?" to "What Are They Doing?", *J. Dent. Res.* 94 (2015) 1628–1637.
- [49] N. Takahashi, B. Nyvad, The role of bacteria in the caries process: ecological perspectives, *J. Dent. Res.* 90 (2011) 294–303.
- [50] M.A.R. Buzalaf, A.R. Hannas, M.T. Kato, Saliva and dental erosion, *J. Appl. Oral Sci.* 20 (2012) 493–502.
- [51] A. Prabhakar, R. Dodawad, R. Os, Evaluation of Flow Rate, pH, Buffering Capacity, Calcium, Total Protein and Total Antioxidant Levels of Saliva in Caries Free and Caries Active Children-An In Vivo Study, *Int. J. Clin. Pediatr. Dent.* 2 (2009) 9–12.
- [52] A.C.R. Tanner, C.A. Kressirer, L.L. Faller, Understanding Caries From the Oral Microbiome Perspective, *J. Calif. Dent. Assoc.* 44 (2016) 437–446.
- [53] A. Georgios, T. Vassiliki, K. Sotirios, Acidogenicity and acidurance of dental plaque and saliva sediment from adults in relation to caries activity and chlorhexidine exposure, *J. Oral Microbiol.* 7 (2015) 26197.
- [54] P.C. Baehni, Y. Takeuchi, Anti-plaque agents in the prevention of biofilm-associated oral diseases, *Oral Dis.* 9 (2003) 23–29.
- [55] S. Jenkins, M. Addy, R. Newcombe, Triclosan and sodium lauryl sulphate mouthwashes (I). Effects on salivary bacterial counts, *J. Clin. Periodontol.* 18 (1991) 140–144.
- [56] S. Shapiro, E. Giertsen, B. Guggenheim, An in vitro oral biofilm model for comparing the efficacy of antimicrobial mouthrinses, *Caries Res.* 36 (2002) 93–100.
- [57] C. van Loveren, Antimicrobial activity of fluoride and its in vivo importance: identification of research questions, *Caries Res.* 35 (2001) 65–70.
- [58] B.R. Charugundla, S. Anjum, M. Mocherla, Comparative effect of fluoride, essential oil and chlorhexidine mouth rinses on dental plaque and gingivitis in patients with and without dental caries: a randomized controlled trial, *Int. J. Dent. Hyg.* 13 (2015) 104–109.

- [59] S. Matthijs, P.A. Adriaens, Chlorhexidine varnishes: a review, *J Clin Periodontol.* 29 (2002) 1–8.
- [60] V. Quintas, I. Prada-Lopez, N. Donos, D. Suarez-Quintanilla, I. Tomas, In situ neutralisation of the antibacterial effect of 0.2% Chlorhexidine on salivary microbiota: Quantification of substantivity, *Arch. Oral Biol.* 60 (2015) 1109–1116.
- [61] I. Tomas, L. Garcia-Caballero, E. Lopez-Alvar, M. Suarez-Cunqueiro, P. Diz, J. Seoane, In situ chlorhexidine substantivity on saliva and plaque-like biofilm: influence of circadian rhythm, *J. Periodontol.* 84 (2013) 1662–1672.
- [62] A. Elworthy, J. Greenman, F.M. Doherty, R.G. Newcombe, M. Addy, The substantivity of a number of oral hygiene products determined by the duration of effects on salivary bacteria, *J. Periodontol.* 67 (1996) 572–576.
- [63] M.C. Cousido, I. Tomas Carmona, L. Garcia-Caballero, J. Limeres, M. Alvarez, P. Diz, In vivo substantivity of 0.12% and 0.2% chlorhexidine mouthrinses on salivary bacteria, *Clin. Oral Investig.* 14 (2010) 397–402.
- [64] I. Goto, S. Furudoi, M. Akashi, T. Komori, Measurement of the Total Number of Bacteria in Saliva Using Quantitative Real-Time PCR During Treatment for Head and Neck Malignancy: A Series of Cases, *Oral Health Dent. Manag.* 14 (2015).

## Figure description

**Fig. 1: Exemplary cytometric 2D-histogram and gate template.** A 2D-histogram created by the generated data of MoFlo measurements is depicted. The two parameters Forward scatter (cell size) vs. DAPI fluorescence (chromosome content) were chosen. A: Cell gate, defined in FlowJo V10 (FlowJo, LLC, Oregon USA) excluding noise and 0.5  $\mu\text{m}$  and 1.0  $\mu\text{m}$  beads, depicted with an exemplary saliva sample (subject 6, taken at baseline for the mouth rinse experiment). For detailed information see 2.8 Data analysis. B: Gate template, generated in FlowJo V10. It consists of 37 gates and must be valid for all samples.

**Fig. 2: Gate dependent variations in cell abundancies, evolution of microbiome structure and similarity analysis.** Two different subjects are compared (subjects 6 and 4). Four samples were collected within 8 h (time points: 0 h, 5 min, 2 h and 8 h). All gates of all samples were used to compare the similarity of the samples. A: Barcodes show in-/decrease of normalized gate cell abundancies. B: The boxplots show the distributions of the relative cell abundancies per gate. C: For a clearer depiction of the changes between two time points (0 h and 5 min), exemplary gates were chosen and colored corresponding to the color key of the barcode that describes lower abundancies (blue color), higher abundancies (red color) or average abundancies (white color). D: NMDS-plots show the evolution of the person's individual salivary microbiome within 8 h. Intra-individual changes are depicted. The size of the dots increases from 0 h up to 8 h. E: Intra- and inter-individual similarity analyses of two persons is demonstrated. Both subjects create their own cluster in this NMDS-plot. The size of these clusters can be used to describe the (dis-) similarity between the samples.

**Fig. 3: Technical replicates and fixation stability.** Dissimilarity analysis of three parallels (including fixation, washing and staining) which were measured three times each as technical replicates (TR) and of fixation stability, measured at days 0, 1, 3, 7, 15, 50, 135 (FIX, open circles in ascending size according to progressive time points). For reference, a long-term experiment (DV) was added: 11 samples of one subject, collected within 3 months (closed circles in ascending size according to progressive time points). The ellipsoids show standard deviations of the sample groups (DV, TR, FIX).

**Fig. 4: Routine workflow for analyzing salivary microbiomes based on flow cytometric measurements.**

In this figure, the experimental design is illustrated schematically. The pilot study implemented ten oral healthy subjects. Unstimulated saliva samples were collected within 3 different experiments: a long-term experiment, testing of sugar and acid influences and the use of bactericide solutions. Single steps of the following processing of the saliva samples within the cytometric workflow are depicted: Fixation procedure enables a stability (for further information see 2.11.2 Fixation stability), so further processing can be delayed if necessary. Once washed and stained with DNA staining solution (DAPI), the flow cytometric community analysis of the samples followed. Duration of measurements can vary from several minutes to nearly half an hour until 150,000 cells per cell gate are detected. Data analysis can be performed immediately by using bioinformatic tools (step by step explanation see 2.8 – 2.9).

**Fig. 5: Intra- and inter-individual microbial cytometric diversity.** The NMDS-plot compares the microbial cytometric diversity of saliva samples collected from 10 subjects, each represented by an individual color. The sampling started at baseline (0h, smallest points) and continued for three months (points increase in size). From each subject 8-11 samples were measured (see Supplementary material Table S1). The larger the distance between two points, the more dissimilar was the cytometric structure of the respective microbial communities. The depiction of the standard deviation occurs by ellipsoids. The expanse of an ellipsoid relates to the intra-individual variability: If it is small, the variability is low. The more distant two ellipsoids are located, the higher is the inter-individual diversity. Stress of the NMDS-plot: 0.12.

**Fig. 6: Effect of sugars and acids on microbial community structures.** The NMDS-plots compare the microbial cytometric diversity of samples collected at baseline (0 h, small points) and after stress (8 h, big points) caused by sugars (A) or acids (B). The color of the points represents the involved subjects (see Fig. 5). The ellipsoids show standard deviations of samples collected at baseline (continuous line) and samples collected after the stress influence (broken line). In both experiments the two ellipsoids show high overlaps, hence no major shifts in respective community structures was caused by the applied stress. Stress values of the NMDS-plots: 0.13 (A), 0.2 (B).

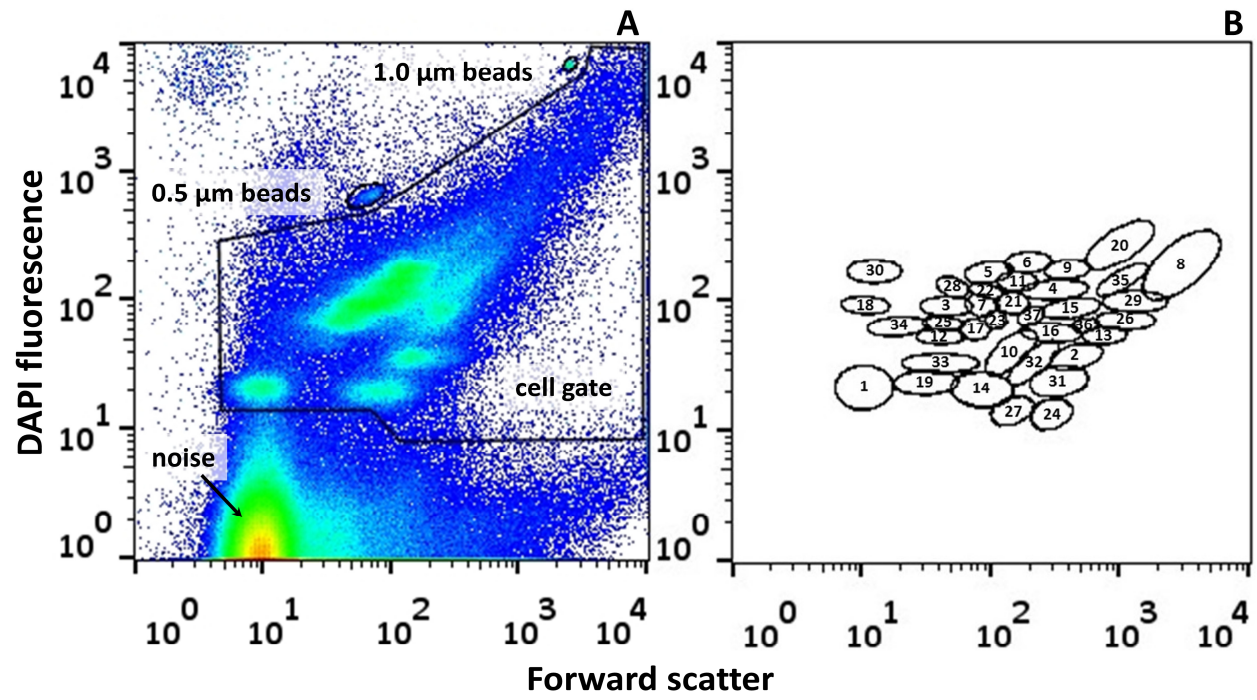
**Fig. 7: Decrease in bacterial cell number after CHX mouth-rinse application.** The cell number of the samples collected at 0 h (baseline), 5 min, 2 h, and 8 h after treatment with 0.2% CHX mouth-rinse is demonstrated per ml and per entire sample amount for two subjects (subjects 6 and 10). All samples show a clear decrease in cell number after 8 h. Both the cell number per entire sample and per ml decreased after rinsing for about 1.8 and 2.6 times (subject 6) and 1.2 and 2.1 times (subject 10), respectively, indicating a successful effect of CHX.

**Fig. 8: Effect of CHX and Listerine® mouth-rinse on microbial community structure.** The NMDS-plots represent the microbial cytometric diversity of saliva samples of five subjects each, who used two different mouth rinses: 0.2 % Chlorhexidine (A) and Listerine® (B). The color of the points represents the involved subjects (see Fig. 5) and the size of the points demonstrates the times of sample collection: baseline (0 h = small points; 5 min = medium small points; 2 h = medium big points; 8 h after rinsing = big points). The respective four areas compare the samples from one collecting time point. The ellipsoids show standard deviations of samples collected at baseline (continuous line), after 5 min (broken line), 2 h (pointed line), and 8 h (mixed line). Both chemicals did not cause noteworthy shifts in the community structure, since there is high overlap of the ellipsoids. Stress values of the NMDS-plots: 0.14 (A), 0.18 (B).

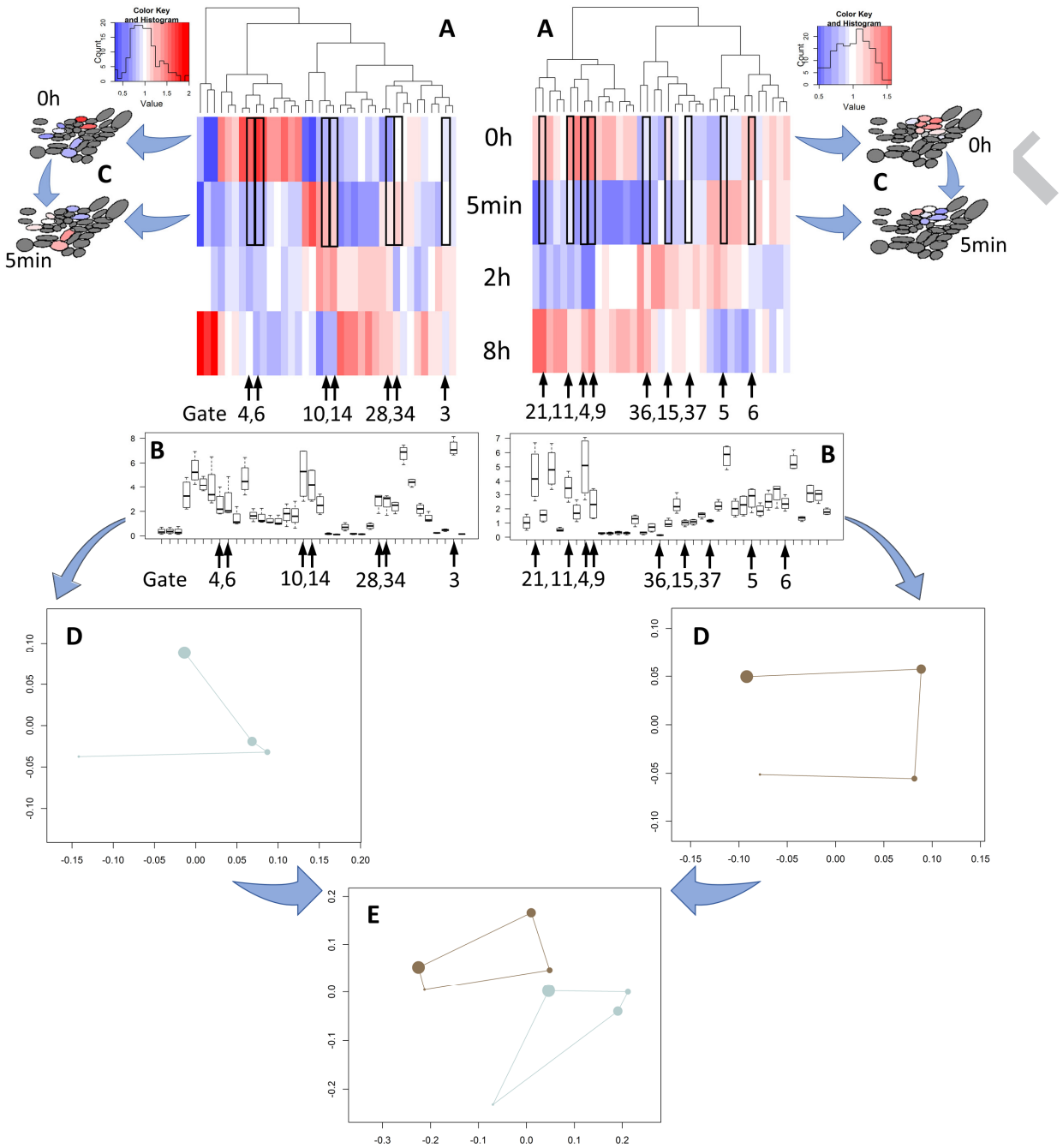
**Fig. 9: Illumina® sequencing of exemplary saliva samples.** The figure depicts the distribution of phylotypes per sample detected by Illumina® sequencing in a way that the colors mark the genera and

the rarefaction curves the OTU numbers. Whole community sequencing as well as sequencing of sorted gates was conducted. Gates for sequencing have been chosen on the basis of increasing and decreasing cell numbers, respectively. A: Samples of the long-term experiment. Sequencing was performed exemplarily for subject 1 (orange) at two different time points (1 week, 4 weeks) as well as subject 6 (blue) and subject 10 (pink) at the same time point (6 weeks). B: Samples of the sugar experiment. Sequencing was performed exemplarily for subject 6 (blue) of samples taken at baseline and after 8 h of stress impact (sugar). In addition, different subsets of the community of subject 6 were sorted such as G3 and G37 (both visible in the 2D-histogram at baseline, but diminished at 8 h), which represented the key phylotypes *Prevotella* and *Alloprevotella*. Other subcommunities showed higher diversity such as G4, G9 (both intensified after the stress impact), and the joint sorting of gates G8, 26 and 29 (all three intensified after the stress impact). C: Samples of the mouth-rinse experiment. Sequencing was performed exemplarily for subject 6 at two different time points (0 h and 8 h after applying 0.2 % CHX mouth-rinse). Cell sorting was performed for the combined gates G5 and G6 (both diminished after the use of mouth-rinse from 11.33 % to 5.25 %), which also evolved as key gate for *Prevotella*. D: To exclude possible distortions by sorting procedure, a sample of subject 6 was split and sequenced unsorted and sorted. Only slight differences become apparent.

ACCEPTED MANUSCRIPT

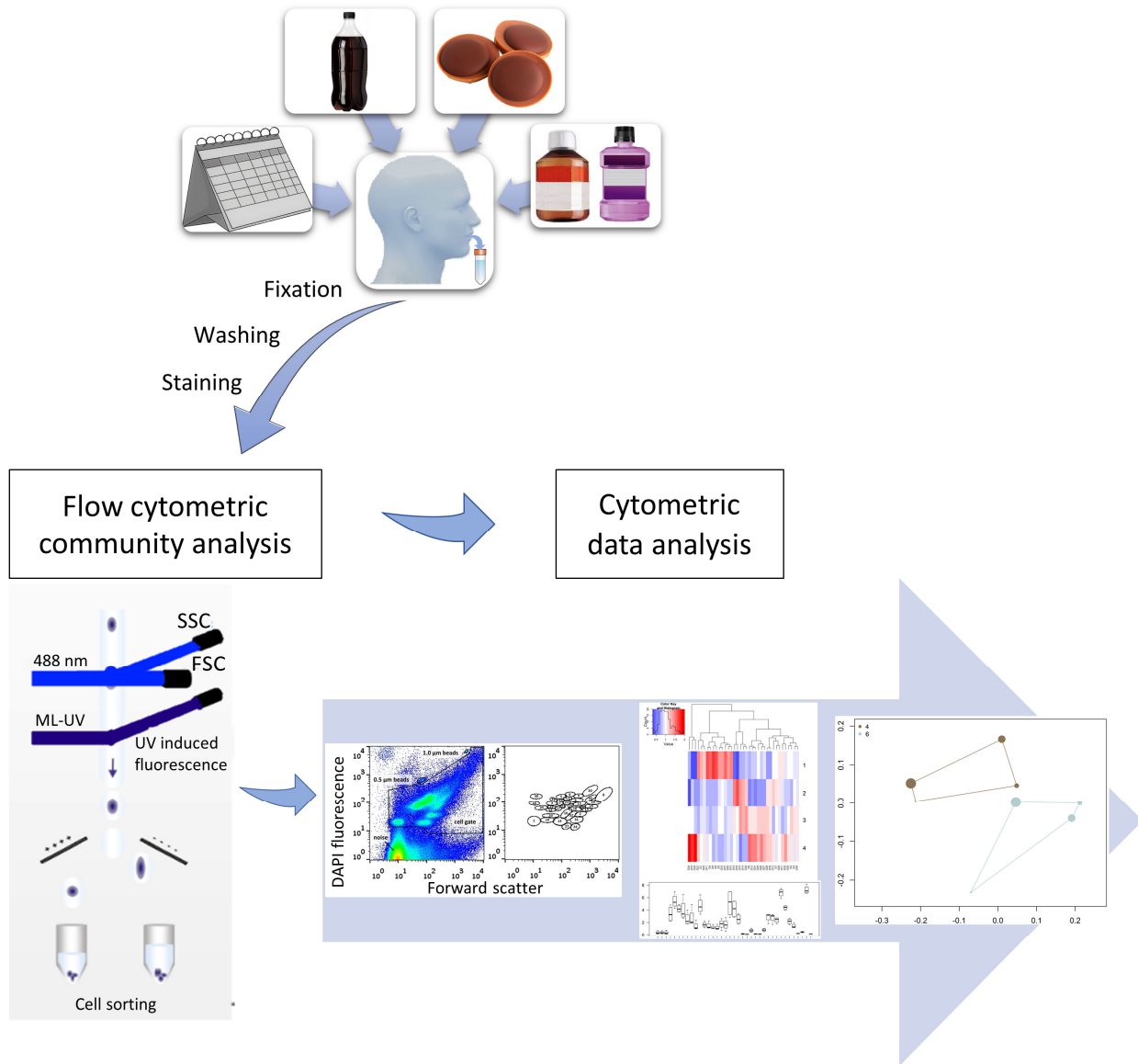


ACCEPTED MANUSCRIPT

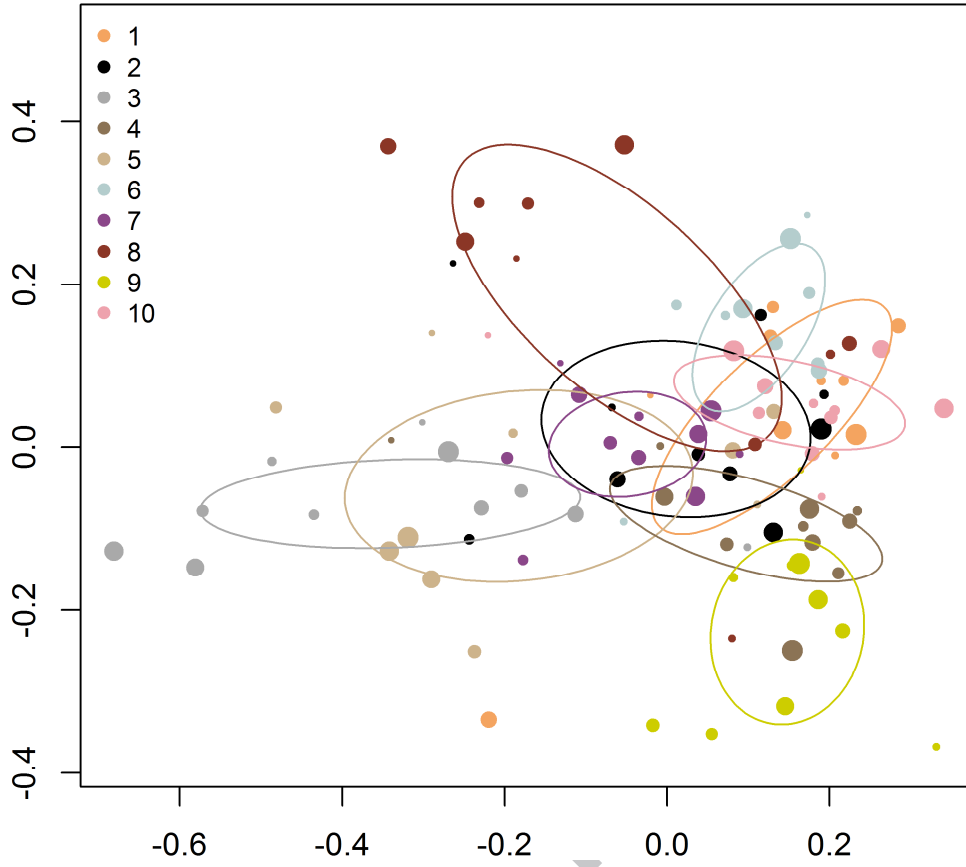


A



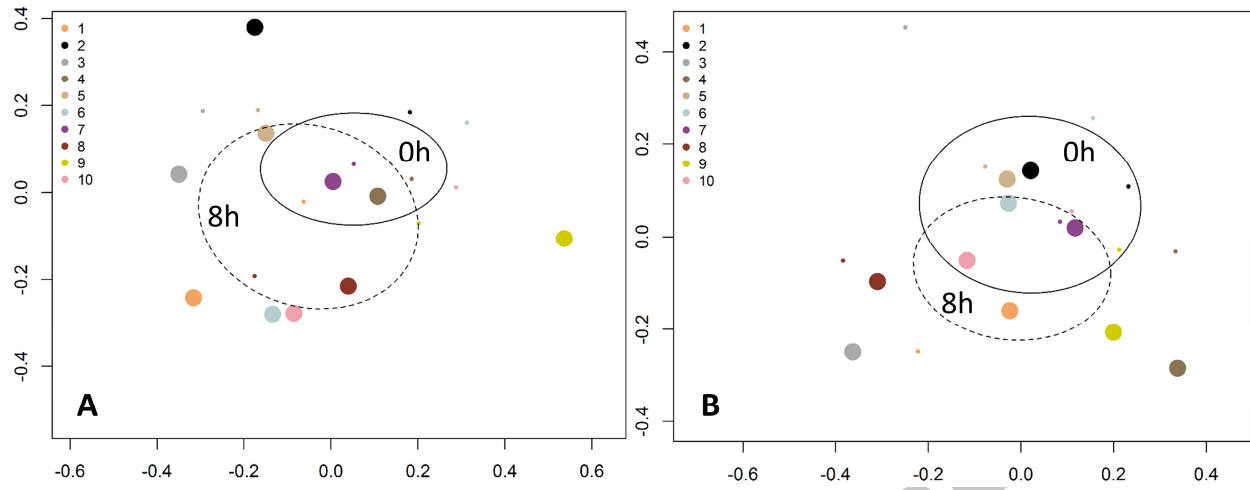


ACCE

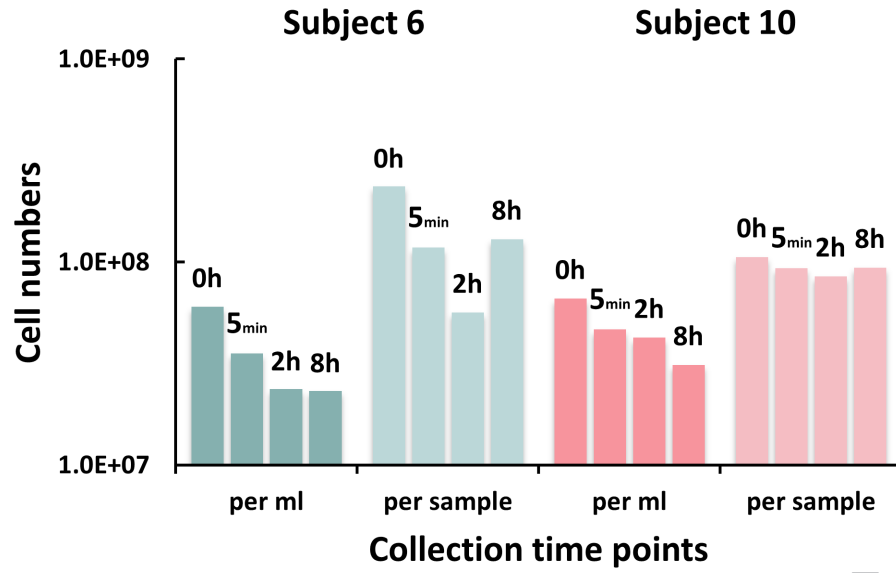


ACCEPTED

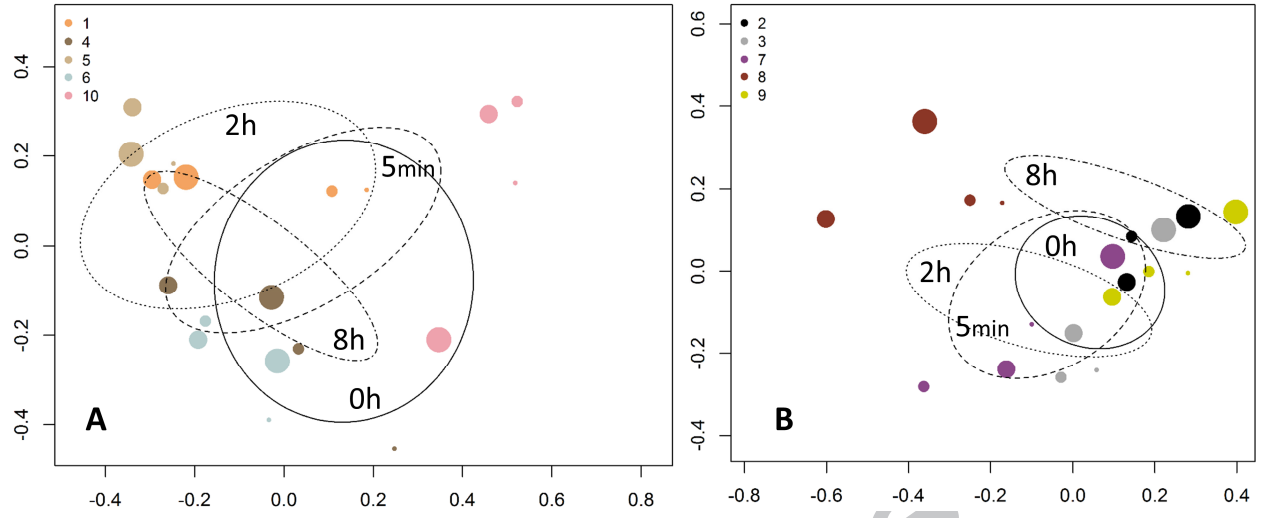
SCRIPT



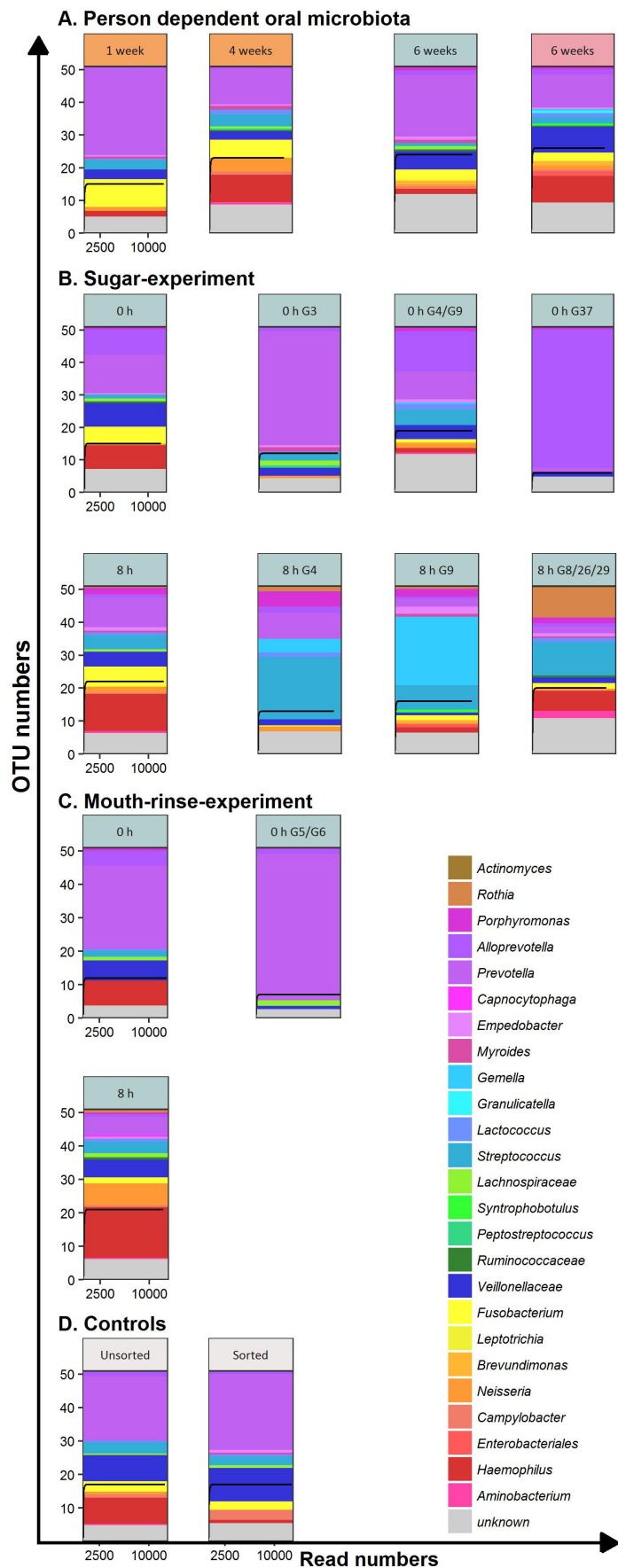
ACCEPTED MANUSCRIPT



ACCEPTED MANUSCRIPT



ACCEPTED MANUSCRIPT



IPT

Highlights for:

## **A cytometric approach to follow variation and dynamics of the salivary microbiota**

- A cytometric workflow for analyzing salivary microbiomes was developed.
- Saliva microbiomes revealed constant profiles with low intra-individual variations but obvious inter-individual diversity in cytometric community structures.
- A short period of sugar- and acid-stress caused no noteworthy changes in the cytometric intra-individual diversity of the various microbiomes.
- Mouth rinse solution caused drastic reductions in bacterial cell counts but no general change in the community composition.

ACCEPTED MANUSCRIPT